

Multiple Antenna Multicast Transmission Assisted by Reconfigurable Intelligent Surfaces

Linsong Du, Jianhui Ma, Qinpeng Liang, and Youxi Tang

Abstract

In order to improve the multiple antenna multicasting in the obstacles environment, a reconfigurable intelligent surface (RIS), which consists of a large number of reconfigurable reflecting elements each being able to reflect the received signals with phase shifts, is set up to assist multicast transmission. Since RIS hardly consumes any energy, it is more environmental-friendly than conventional relaying mode. This paper considers a multicast transmission assisted by the RIS, i.e., a multiple-antennas base station (BS) sends the common messages to K single-antenna mobile users (MUs), where an RIS is deployed as an amplify-and-forward no-power relay to assist this transmission. An equivalent channel model for the considered multicast system is analyzed, and then a capacity maximization problem is formulated to obtain the optimal covariance matrix of the transmitted symbol vector and phase shifts of RIS, which is a non-convex non-differentiable problem. First, we consider this problem for a special scenario, i.e., $K = 2$, which owns three differentiable cases, and the optimal solutions for the three cases are obtained by KKT conditions and a proposed numerical algorithm, respectively. Then, for $K > 2$, since the maximization problem is non-differentiable, this paper reformulates this problem as a differentiable problem, and proposes two numerical algorithms, i.e., subgradient and gradient descent methods, to approach the optimal solution. Finally, in order to more intuitively comprehend the performances of RIS in multicast transmission, the order growth of the maximum capacity of the considered multicast system is obtained in the scenarios that the numbers of reflecting elements, BS antennas, and MUs go to infinity.

Index Terms

Reconfigurable intelligent surfaces (RIS), multiple antenna multicast transmission, multiple mobile users (MUs), phase shift, covariance matrix, capacity maximization.

L. Du, J. Ma, Q. Liang, and Y. Tang are with the National Key Laboratory of Science and Technology on Communications, University of Electronic Science and Technology of China, Chengdu, China, 611731. Emails: llinsongdu@std.uestc.edu.cn.

I. INTRODUCTION

Reconfigurable intelligent surface (RIS) technology has received widespread attentions in wireless communications in the recent years. The RIS consists of a large number of reconfigurable reflecting elements, each of which can induce the phase shifts of the received signals and then reflects them. RIS can provide a new link to maintain transmissions [1] in the indoor and outdoor environments, where the direct paths between the base station (BS) and mobile users (MUs) is blocked by obstacles [2], [3]. It is worth noting that RIS can be seen as no-power multiple input multiple output full-duplex (FD) amplify-and-forward (AF) relay which receives signals and then forwards them to MUs. However, there are some differences between the AF relay and the RIS. Since the RIS hardly consumes any energy, it leads much more energy efficiency and environment-friendly than regular FD AF relay [4]. In the other hand, comparing with FD relay, RIS does not generate self-interference. Moreover, due to the fact that RIS owns less complex structure and low-cost, it is easily to densely set up on a lot of places such as trees, buildings, and rooms [5].

A. Related Works

Considering the above advantages, some works [6]–[15] have researched the application of the RIS in wireless communications. The authors in [6]–[9] considered the scenarios that the BS serves one MU. In [6], an RIS assisted large-scale antenna system was considered, where the direct path between the BS and MUs is blocked by obstacles, and the authors studied the effect of the phase shifts on the ergodic capacity in different propagations. In [7], the authors considered the direct path existing case, and maximized the total received signal power by jointly optimizing the transmit beamforming and the phase shifts for BS and RIS, respectively. In [8], the authors maximized the average achievable rate for an RIS-assisted unmanned aerial vehicles communication system by successive convex approximation method. In [9], the authors compared performances of the RIS and AF relay in the single MUs scenario, discussing the key differences and similarities between them.

The authors in [10]–[13] studied the RIS in downlink communication network, where a BS transmits signals to the multiple MUs assisted by the RIS, and the MUs required messages are different. In [10], the authors minimized the total transmit powers for the RIS enhanced downlink communication network by jointly optimizing the transmit beamforming and the phase shifts.

The authors in [11] studied RIS in non-orthogonal multiple access (NOMA) downlink communication, where the MUs are grouped into multiple clusters, and each of clusters apply NOMA protocol during transmission. The authors in [12] studied the energy efficiency for download communications network assisted by RIS, and formulated an energy efficiency maximization problem [12] to optimize the phase shifts of RIS and the transmit power. In [13], the authors studied the RIS in simultaneous wireless information and power transfer system, where the BS sends both information and energy signals to the multiple MUs assisted by RIS.

In future 5G wireless networks, the demands of sending common messages, such as music sharing, video streaming, and downloading pictures, to multiple MUs will continue to grow [16]. Multiple antenna multicast transmission is a perfectly application for sending the common messages to MUs with high transmission rate [17]. Comparing with the unicast transmissions, i.e., the base station (BS) only servers one MU during one time slot, the multicast transmission can significantly reduce the energy consumption and save the spectrum resource [17]. RIS in multicast transmission also has received interest [14], [15]. The authors in [14] considered the max-min multicast transmission fair quality of service for multicast assisted by RIS, and proposed the efficient algorithms to optimize the quality of service by jointly designing the transmit beamforming and phase shifts. The authors in [15] considered the multi-group multicasting assisted by RIS, and maximized the sum rate of all the multicasting groups by optimizing the transmit beamforming and phase shift of RIS. However, to the best of our knowledge, there is no work considering the capacity of multiple-antenna multicast assisted by RIS, which is a basic and significant problem.

B. Summary of Main Results

In this paper, we consider multiple antenna multicast transmission assisted by RIS. A multiple-antennas BS sends the common messages to multiple single-antenna MUs. Since the direct paths between the BS and MUs are blocked by the obstacles, an RIS consisting of a large number of reconfigurable reflecting elements is set up to assist the multicast transmission, where the BS sends the signals to the RIS, and then the RIS forwards the received signals to the multiple MUs with phase shifts, and the channel state information (CSI) for the links from the BS to the RIS and from the RIS to the MUs are perfectly known to the BS and RIS. The equivalent channel model for the considered multicast system is obtained, which can be seen as a conventional multicast channel, and the characteristics of this multicast channel can be partly controlled by the reconfigurable reflecting elements. Thus, it is crucial to find the optimal phase shifts of RIS

for maximizing the capacity of this equivalent model. The main contributions of this paper are summarized as follows.

- First, a capacity maximization problem is formulated to obtain the optimal phase shifts for RIS and corresponding covariance matrix of the transmitted symbol vector in a two MUs scenario, which is a non-differentiable max-min problem. Thus, we discuss the three cases for this problem, each of which is differentiable. The optimal solutions for the three cases are obtained by KKT conditions and a proposed numerical algorithm, respectively.
- Next, we generalize this capacity maximization problem to the multiple MUs scenario. Since this problem is non-convex and non-differentiable, it is different to directly obtain the optimal solution. Thus, we reformulate non-differentiable problem to a differentiable problem, and then obtain the necessary conditions that optimal solution needs to satisfy. Then, we propose the two numerical algorithms, i.e., subgradient and gradient descent methods, to approach the optimal solution.
- Last, the solutions from numerical algorithms will lose intuitions for the performance of RIS in transmission. Thus, we analyze the order growth of the maximum capacity of the multicast transmission assisted by RIS in the scenarios; 1) The number of MUs is fixed, and the numbers of BS antennas or reflecting elements are taken to infinity; 2) The numbers of BS antennas and reflecting elements are fixed, and the number of MUs is taken to infinity; 3) The numbers of BS antennas, reflecting elements, and MUs all go to infinity.

The structure of this paper is organized as follows. Section II introduces the system model of RIS in multicast transmission, and formulates a capacity maximization problem. Section III obtains the optimal solution for the maximization problem in two MUs scenario. Section IV extends to the results to the multiple MUs scenario. Section V shows the asymptotic analysis for the capacity of the multicast transmission assisted by RIS. Section VI presents the numerical results. Section VII concludes our works.

II. SYSTEM MODEL AND PROBLEM FORMULATION

A. System Model

As shown in Fig. 1, a M -antennas BS sends the common messages to K single-antenna MUs. The direct links between the BS and MUs are blocked by the obstacles. However, since the plenty of scatters fills the wireless environment, we consider to set up an RIS with N reflecting elements between the BS and K MUs to provide a new links maintaining transmission, where

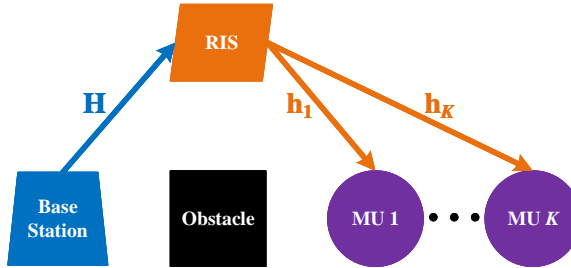


Fig. 1: multicast transmissions assisted by RIS with K MUs.

CSI is perfectly known to the BS and the RIS. Accordingly, the received signal at MU k , $k = 1, 2, \dots, K$ is given as

$$y_k = \mathbf{h}_k^H \Phi \mathbf{H} \mathbf{s} + z_k, \quad (1)$$

where $\mathbf{s} = [s_1, s_2, \dots, s_M]^T$ is the transmitted symbol vector; $\mathbf{H} \in \mathbb{C}^{N \times M}$ is the channel coefficients matrix between the BS and the RIS, i.e.,

$$\mathbf{H} = \begin{bmatrix} H_{1,1} & H_{1,2} & \cdots & H_{1,M} \\ H_{1,2} & H_{2,2} & \cdots & H_{2,M} \\ \vdots & \vdots & \ddots & \vdots \\ H_{1,N} & H_{2,N} & \cdots & H_{N,M} \end{bmatrix}, \quad (2)$$

with $H_{n,m} = a_{H_{n,m}} e^{j\theta_{H_{n,m}}}$; $\mathbf{h}_k^H \in \mathbb{C}^{1 \times N}$ is the channel coefficients vector between the RIS and the MU k , i.e.,

$$\mathbf{h}_k^H = [h_{k,1}, h_{k,2}, \dots, h_{k,N}], \quad (3)$$

with $h_{k,n} = a_{h_{k,n}} e^{j\theta_{h_{k,n}}}$; $\Phi = \text{diag}[\phi_1, \phi_2, \dots, \phi_N] \in \mathbb{C}^{N \times N}$ is a diagonal matrix representing the phase shifts via the reflecting element on the RIS, with $\phi_n = e^{j\theta_n}$, $\theta_n \in [0, 2\pi]$, $n = 1, 2, \dots, N$; and z_k is the circularly symmetric complex Gaussian (CSCG) noise with zero mean and unit variance $\sigma^2 = 1$.

Remark 2.1: From (1), we observe that the RIS shift the phase at the received signal $\mathbf{H} \mathbf{s}$, which is similar to a no-power AF relay [12]. Moreover, $\mathbf{h}_k^H \Phi \mathbf{H}$ is an equivalent downlink channel coefficients matrix [15] between the BS and MU k , and the channel characteristics of

¹ $\{\cdot\}^T$ denotes transposition and $\{\cdot\}^H$ denotes conjugate transposition.

the equivalent channel is partly controlled by phase shifts $\boldsymbol{\theta} = [\theta_1, \theta_2, \dots, \theta_N]$.

B. Problem Formulation

From Remark 2.1, it is obvious that for the fixed Φ the capacity of the equivalent multicast channel is given as [15]

$$C(\Phi) \equiv \max_{\mathbf{Q}: \mathbf{Q} \succ 0, \text{Tr}(\mathbf{Q}) \leq P_{\max}} \min_{k=1, \dots, K} \log (1 + \mathbf{h}_k^H \Phi \mathbf{H} \mathbf{Q} \mathbf{H}^H \Phi^H \mathbf{h}_k), \quad (4)$$

where $\mathbf{Q} = \mathbb{E} \{ \mathbf{s} \mathbf{s}^H \}$ is the covariance matrix of the transmitted symbol vector \mathbf{s} ; $\text{Tr}(\cdot)$ denotes the trace of a matrix; P_{\max} is power budget, and thus $\text{Tr}(\mathbf{Q}) \leq P_{\max}$ is power constraint.

From (4), it is observed that the capacity is varied with Φ . In order to obtain the maximum capacity for the equivalent multicast channel by jointly optimizing the covariance matrix \mathbf{Q} and phase shifts $\boldsymbol{\theta} = [\theta_1, \theta_2, \dots, \theta_N]$, a maximization problem is formulated as

$$(P1) \quad C^* = \max_{\mathbf{Q}, \boldsymbol{\theta}} \min_{k=1, \dots, K} \log (1 + \mathbf{h}_k^H \Phi \mathbf{H} \mathbf{Q} \mathbf{H}^H \Phi^H \mathbf{h}_k) \quad (5)$$

$$\text{s.t. } \text{Tr}(\mathbf{Q}) \leq P_{\max}, \quad (6)$$

$$\mathbf{Q} \succ 0, \quad (7)$$

$$\theta_n \in [0, 2\pi], n = 1, 2, \dots, N. \quad (8)$$

It is obvious that the objective function (5) is a non-convex due to the phase shifts [18], and thus Problem (P1) is non-convex. In general, there is no effective and standard method to solve the non-convex problem. Moreover, the objective function (5) is non-differentiable due to the fact the pointwise minimum $\min \{\cdot\}$ is non-differentiable [18], and therefore the KKT conditions² of Problem (P1) are also non-existent [18]. Thus, we first consider $K = 2$ for Problem (P1), in which the objective function (5) is reformulated as a differentiable function, and then we generalize to $K > 2$ in next.

²KKT conditions are the necessary conditions that optimal solutions need to satisfy for a differentiable problem

III. OPTIMAL SOLUTION FOR THE CASE OF $K = 2$

In this section, we consider $K = 2$, i.e., two MUs scenario, for Problem (P1). For $K = 2$, Problem (P1) can be rewritten as

$$\begin{aligned} (\text{P2}) \quad & \max_{\mathbf{Q}, \boldsymbol{\theta}} \min \{R_1(\mathbf{Q}, \boldsymbol{\theta}), R_2(\mathbf{Q}, \boldsymbol{\theta})\} \\ & \text{s.t. (6), (7), (8).} \end{aligned} \quad (9)$$

where $R_k(\mathbf{Q}, \boldsymbol{\theta})$, $k = 1, 2$, are defined as

$$R_k(\mathbf{Q}, \boldsymbol{\theta}) = \log \left(1 + \mathbf{h}_k^H \boldsymbol{\Phi} \mathbf{H} \mathbf{Q} \mathbf{H}^H \boldsymbol{\Phi}^H \mathbf{h}_k \right). \quad (10)$$

In order to solve Problem (P2), a specialized technique for max-min problem is introduced as follows, which is showed in [19] in detail.

First, we define the following function:

$$\begin{aligned} V(\epsilon) &= \max_{(\mathbf{Q}, \boldsymbol{\theta}) \in \mathcal{Q}} R(\mathbf{Q}, \boldsymbol{\theta}, \epsilon) \\ &= \max_{(\mathbf{Q}, \boldsymbol{\theta}) \in \mathcal{Q}} \{ \epsilon R_1(\mathbf{Q}, \boldsymbol{\theta}) + (1 - \epsilon) R_2(\mathbf{Q}, \boldsymbol{\theta}) \}, \quad 0 \leq \epsilon \leq 1, \end{aligned} \quad (11)$$

where $\mathcal{Q} = \{(\mathbf{Q}, \boldsymbol{\theta}) | (6), (7), (8)\}$ is the feasible set for Problem (P2). Here, we define that $(\mathbf{Q}_\epsilon, \boldsymbol{\theta}_\epsilon)$ is the optimal solution of $\max_{(\mathbf{Q}, \boldsymbol{\theta}) \in \mathcal{Q}} R(\mathbf{Q}, \boldsymbol{\theta}, \epsilon)$ for fixed ϵ , i.e.,

$$V(\epsilon) = R(\mathbf{Q}_\epsilon, \boldsymbol{\theta}_\epsilon, \epsilon). \quad (12)$$

Then, based on [19], we obtain the following lemma.

Lemma 3.1: If ϵ^* is the optimal solution for $\min_{0 \leq \epsilon \leq 1} V(\epsilon)$, $(\mathbf{Q}_{\epsilon^*}, \boldsymbol{\theta}_{\epsilon^*})$ is the optimal solution for Problem (P2). The relationship between $R_1(\mathbf{Q}_{\epsilon^*}, \boldsymbol{\theta}_{\epsilon^*})$ and $R_2(\mathbf{Q}_{\epsilon^*}, \boldsymbol{\theta}_{\epsilon^*})$ is summarized as the following three cases:

- Case 1: If $\epsilon^* = 0$, it follows $R_1(\mathbf{Q}_{\epsilon^*}, \boldsymbol{\theta}_{\epsilon^*}) \geq R_2(\mathbf{Q}_{\epsilon^*}, \boldsymbol{\theta}_{\epsilon^*})$;
- Case 2: If $\epsilon^* = 1$, it follows $R_1(\mathbf{Q}_{\epsilon^*}, \boldsymbol{\theta}_{\epsilon^*}) \leq R_2(\mathbf{Q}_{\epsilon^*}, \boldsymbol{\theta}_{\epsilon^*})$;
- Case 3: If $0 < \epsilon^* < 1$, it follows $R_1(\mathbf{Q}_{\epsilon^*}, \boldsymbol{\theta}_{\epsilon^*}) = R_2(\mathbf{Q}_{\epsilon^*}, \boldsymbol{\theta}_{\epsilon^*})$.

Based on Lemma (3.1), we discuss the three cases respectively in next.

Case1: We first consider Case 1. Due to the symmetry, the results of Case 1 are easy to generalize that of Case 2.

When Case 1 occurs, i.e., $\epsilon^* = 0$, it is obvious that $\{\mathbf{Q}_0, \boldsymbol{\theta}_0\}$ is optimal solution for Problem (P2), and condition $R_1(\mathbf{Q}_0, \boldsymbol{\theta}_0) \geq R_2(\mathbf{Q}_0, \boldsymbol{\theta}_0)$ must be satisfied. Thus, we must solve the following problem to obtain $\{\mathbf{Q}_0, \boldsymbol{\theta}_0\}$:

$$R_2(\mathbf{Q}_0, \boldsymbol{\theta}_0) = \max_{(\mathbf{Q}, \boldsymbol{\theta}) \in \mathcal{Q}} \log (1 + \mathbf{h}_2^H \Phi \mathbf{H} \mathbf{Q} \mathbf{H}^H \Phi^H \mathbf{h}_2). \quad (13)$$

Based on [15], we obtain

$$\begin{aligned} & \max_{(\mathbf{Q}, \boldsymbol{\theta}) \in \mathcal{Q}} \log (1 + \mathbf{h}_2^H \Phi \mathbf{H} \mathbf{Q} \mathbf{H}^H \Phi^H \mathbf{h}_2) \\ & \equiv \max_{\boldsymbol{\theta} \in \mathcal{Q}} \log \left(1 + P_{\max} \|\mathbf{h}_2^H \Phi \mathbf{H}\|^2 \right), \end{aligned} \quad (14)$$

and the optimal power \mathbf{Q}_0 is given as

$$\mathbf{Q}_0 = \mathbf{V}_0^H \text{diag} [P_{\max}, 0, \dots, 0] \mathbf{V}_0, \quad (15)$$

where $\mathbf{V}_0 \in \mathbb{C}^{N \times N}$ is obtained from the singular value decomposition of $\mathbf{h}_2^H \Phi_0 \mathbf{H}$, i.e.,

$$\mathbf{h}_2^H \Phi_0 \mathbf{H} \equiv \mathbf{U}_0 \Sigma_0 \mathbf{V}_0^H, \quad (16)$$

$\mathbf{U}_0 = 1$, \mathbf{V}_0^H are unitary matrices, and $\Sigma_0 \in \mathbb{C}^{1 \times N}$ is a rectangular matrix.

Remark 3.1: From (14), (15) and (16), it is observed that we only need to compute $\boldsymbol{\theta}_0$ by maximizing $\log \left(1 + P_{\max} \|\mathbf{h}_2^H \Phi \mathbf{H}\|^2 \right)$. After obtaining $\boldsymbol{\theta}_0$, \mathbf{Q}_0 can be obtained by (15) and (16).

Thus, we only need to solve the following problem

$$(P2.1) \max_{\boldsymbol{\theta}: \theta_n \in [0, 2\pi], n=1, 2, \dots, N} \|\mathbf{h}_2^H \Phi \mathbf{H}\|^2. \quad (17)$$

Then, the optimal solution $\boldsymbol{\theta}_0$ for Problem (P2.1) is summarized in the following proposition.

Proposition 3.1: The necessary conditions that optimal solution $\boldsymbol{\theta}_0 = [\theta_{0,1}, \dots, \theta_{0,N}]$ needs to

satisfy for Problem (P2.1) is given as

$$\begin{aligned}
0 &= \sum_{m=1}^M \sum_{j=1, j \neq n}^N 2G_{n,j,m}^{(2)} \sin \left(\theta_{0,n} - \theta_{0,j} + \vartheta_{n,j,m}^{(2)} \right) + \lambda_{n,1} - \lambda_{n,2}, \\
0 &= \lambda_{n,1} (\theta_{0,n} - 2\pi), \quad 0 = -\lambda_{n,2} \theta_{0,n}, \\
0 \leq \theta_{0,n} &\leq 2\pi, \quad \lambda_{n,1} \geq 0, \quad \lambda_{n,2} \geq 0, \\
n &= 1, \dots, N,
\end{aligned} \tag{18}$$

where $G_{n,j,m}^{(2)} = a_{h_{2,n}} a_{h_{2,j}} a_{H_{n,m}} a_{H_{j,m}}$ and $\vartheta_{n,j,m}^{(2)} = \theta_{h_{2,n}} - \theta_{h_{2,j}} + \theta_{H_{n,m}} - \theta_{H_{j,m}}$

Proof: Please see Appendix A. ■

Remark 3.2: From Proposition 3.1, we obtain that

- The optimal solution $\boldsymbol{\theta}_0$ for Problem (P2.1) is a root of the system of equations (18), which can be obtained by the interval iterative method [20].
- Proposition 3.1 only obtain the necessary conditions that optimal solution needs to satisfy. In order to gain insight, we consider a special case, i.e., $N = 2$, for Problem (P2.1), which owns the closed-form solution.

From the proof of Proposition 3.1, Problem (P2.1) for $N = 2$ can be rewritten as

$$\max_{\boldsymbol{\theta}: \theta_n \in [0, 2\pi], n=1,2} \sum_{m=1}^M 2G_{1,2,m}^{(2)} \cos \left(\theta_1 - \theta_2 + \vartheta_{n,j,m}^{(2)} \right) \tag{19}$$

$$= \max_{\boldsymbol{\theta}: \theta_n \in [0, 2\pi], n=1,2} 2\bar{G}_{1,2}^{(2)} \cos \left(\theta_1 - \theta_2 + \bar{\vartheta}_{1,2}^{(2)} \right), \tag{20}$$

where $\bar{\vartheta}_{1,2}^{(2)} \in [0, 2\pi]$ is the auxiliary angle of $\vartheta_{n,j,m}^{(2)}$, $m = 1, \dots, M$. It is obvious that $\theta_1 - \theta_2 - \bar{\vartheta}_{1,2}^{(2)} = 0$ is optimal for (20). Thus, is optimal solution for Problem (P2.1) is given as

$$\left\{ \boldsymbol{\theta}_0 : \theta_{0,1} - \theta_{0,2} = \bar{\vartheta}_{1,2}^{(2)}, \theta_{0,n} \in [0, 2\pi], n = 1, 2 \right\} \tag{21}$$

Final, we can obtain the \mathbf{Q}_0 by (15) and $\boldsymbol{\theta}_0$.

Case2: When Case 2 occurs, i.e., $\epsilon^* = 1$, it is obvious that $\{\mathbf{Q}_1, \boldsymbol{\theta}_1\}$ is optimal solution for Problem (P2), and condition $R_1(\mathbf{Q}_1, \boldsymbol{\theta}_1) \leq R_2(\mathbf{Q}_1, \boldsymbol{\theta}_1)$ must be satisfied. By the same idea of Case 1, we only need to solve the following problem

$$(\text{P2.2}) \quad \max_{\boldsymbol{\theta}: \theta_n \in [0, 2\pi], n=1,2, \dots, N} \|\mathbf{h}_1^H \boldsymbol{\Phi} \mathbf{H}\|^2. \tag{22}$$

The optimal solution $\boldsymbol{\theta}_1$ for Problem (P2.2) is summarized in the following proposition.

Proposition 3.2: The necessary conditions that the optimal solution $\boldsymbol{\theta}_1 = [\theta_{1,1}, \dots, \theta_{1,N}]$ needs to satisfy for Problem (P2.2) is given as

$$\begin{aligned} 0 &= \sum_{m=1}^M \sum_{j=1, j \neq n}^N 2G_{n,j,m}^{(1)} \sin \left(\theta_{1,n} - \theta_{1,j} + \vartheta_{n,j,m}^{(1)} \right) + \lambda_{n,1} - \lambda_{n,2} \\ 0 &= \lambda_{n,1} (\theta_{1,n} - 2\pi), \quad -\lambda_{n,2} \theta_{1,n}, \\ 0 \leq \theta_{1,n} &\leq 2\pi, \quad \lambda_{n,1} \geq 0, \quad \lambda_{n,2} \geq 0, \\ n &= 1, \dots, N, \end{aligned} \quad (23)$$

where $G_{n,j,m}^{(1)} = a_{h_{1,n}} a_{h_{1,j}} a_{H_{n,m}} a_{H_{j,m}}$ and $\vartheta_{n,j,m}^{(1)} = \theta_{h_{1,n}} - \theta_{h_{1,j}} + \theta_{H_{n,m}} - \theta_{H_{j,m}}$.

Proof: This proof is same to that of Proposition 3.1, and thus is omitted for brevity. ■

Then, we can obtain the \mathbf{Q}_1 by (23) and the obtained $\boldsymbol{\theta}_1$.

Case3: When Case 3 occurs, i.e., $0 < \epsilon^* < 1$, it follows that $\{\mathbf{Q}_{\epsilon^*}, \boldsymbol{\theta}_{\epsilon^*}\}$ is optimal solution for Problem (P2), and condition $R_1(\mathbf{Q}_{\epsilon^*}, \boldsymbol{\theta}_{\epsilon^*}) = R_2(\mathbf{Q}_{\epsilon^*}, \boldsymbol{\theta}_{\epsilon^*})$ must be satisfied. Based on (11), we formulate

$$(P2.3) \quad \max_{(\mathbf{Q}, \boldsymbol{\theta}) \in \mathcal{Q}} \epsilon^* R_1(\mathbf{Q}, \boldsymbol{\theta}) + (1 - \epsilon^*) R_2(\mathbf{Q}, \boldsymbol{\theta}), \quad (24)$$

to obtain $\{\mathbf{Q}_{\epsilon^*}, \boldsymbol{\theta}_{\epsilon^*}\}$.

For Problem (P2.3), we first show the necessary conditions that optimal solution $\{\mathbf{Q}_{\epsilon^*}, \boldsymbol{\theta}_{\epsilon^*}\}$ needs to satisfy for Problem (P2.3) by the KKT conditions, which indicates the structure of optimal solution $\{\mathbf{Q}_{\epsilon^*}, \boldsymbol{\theta}_{\epsilon^*}\}$, and then propose a numerical algorithm to approach the optimal solution.

A. Necessary Conditions of Optimal Solution for Case 3

Lagrangian [18] of Problem (P2.3) is given as

$$\begin{aligned} L(\mathbf{Q}, \boldsymbol{\theta}) &= -\epsilon^* R_1(\mathbf{Q}, \boldsymbol{\theta}) - (1 - \epsilon^*) R_2(\mathbf{Q}, \boldsymbol{\theta}) + \mu (\text{Tr}(\mathbf{Q}) - P_{\max}) - \text{Tr}(\boldsymbol{\Psi} \mathbf{Q}) \\ &\quad + \sum_{n=1}^N \lambda_{n,1} (\theta_n - 2\pi) - \sum_{n=1}^N \lambda_{n,2} \theta_n, \end{aligned} \quad (25)$$

where μ , $\boldsymbol{\Psi}$, $\lambda_{n,1}$, and $\lambda_{n,2}$, $n = 1, \dots, N$ are Lagrangian multipliers.

By taking the derivative of the function $L(\mathbf{Q}, \boldsymbol{\theta})$, KKT conditions that Problem (2.3) needs to satisfy are given as

$$\begin{aligned}\nabla_{\mathbf{Q}} L &= -\epsilon^* \frac{\mathbf{H}^H \Phi^H \mathbf{h}_1 \mathbf{h}_1^H \Phi \mathbf{H}}{1 + \mathbf{h}_1^H \Phi \mathbf{H} \mathbf{Q} \mathbf{H}^H \Phi^H \mathbf{h}_1} - (1 - \epsilon^*) \frac{\mathbf{H}^H \Phi^H \mathbf{h}_2 \mathbf{h}_2^H \Phi \mathbf{H}}{1 + \mathbf{h}_2^H \Phi \mathbf{H} \mathbf{Q} \mathbf{H}^H \Phi^H \mathbf{h}_2} + \mu \mathbf{I} - \boldsymbol{\Phi} = \mathbf{0}, \\ \nabla_{\boldsymbol{\theta}} L &= -\epsilon^* \frac{\Delta_1 \mathbf{H} \mathbf{Q} \mathbf{H}^H \Delta_1^H \boldsymbol{\varphi}}{1 + \mathbf{h}_1^H \Phi \mathbf{H} \mathbf{Q} \mathbf{H}^H \Phi^H \mathbf{h}_1} - (1 - \epsilon^*) \frac{\Delta_2 \mathbf{H} \mathbf{Q} \mathbf{H}^H \Delta_2^H \boldsymbol{\varphi}}{1 + \mathbf{h}_2^H \Phi \mathbf{H} \mathbf{Q} \mathbf{H}^H \Phi^H \mathbf{h}_2} + \boldsymbol{\lambda}_1 - \boldsymbol{\lambda}_2 = \mathbf{0}, \\ P_{\max} &\geq \text{Tr}(\mathbf{Q}), \quad \mathbf{Q} \succeq \mathbf{0}, \quad \mu \geq 0, \quad \boldsymbol{\Phi} \succeq \mathbf{0}, \quad 0 = \mu (\text{Tr}(\mathbf{Q}) - P_{\max}), \quad \mathbf{0} = \boldsymbol{\Phi} \mathbf{Q}, \\ \lambda_{n,1} (\theta_n - 2\pi) &= 0, \quad -\lambda_{n,2} \theta_n = 0, \quad 0 \geq \theta_n \geq 2\pi, \quad \lambda_{n,1} \geq 0, \quad \lambda_{n,2} \geq 0, \quad n = 1, \dots, N, \end{aligned}\quad (26)$$

where $\boldsymbol{\varphi} = [je^{j\theta_1}, \dots, je^{j\theta_N}]^T$, $\Delta_k = \text{diag}[h_{k,1}, \dots, h_{k,N}]$, $\boldsymbol{\lambda}_1 = [\lambda_{1,1}, \dots, \lambda_{1,N}]^T$, $\boldsymbol{\lambda}_2 = [\lambda_{2,1}, \dots, \lambda_{2,N}]^T$, and \mathbf{I} is unit matrix.

The KKT condition (26) indicates the structure of the optimal solution for Problem (P2.4); however, it is complex to compute the optimal solution for Problem (P2.4) by solving equations (26). Therefore, we propose a numerical algorithm to compute the optimal solution for Problem (P2.4).

B. Numerical Algorithm for Case 3

Since Problem (2.3) is an inequality constrained optimization problem and continuously differentiable, we perform the logarithmic barrier methods [18] to converge the objective function of Problem (P2.3) as a local optimum.

First, we reformulate the inequality constrained Problem (P2.3) as an unconstrained minimization problem

$$(\text{P2.3}^*) \quad \min \Gamma_1^{(t)}(\mathbf{Q}, \boldsymbol{\theta}), \quad (27)$$

where $\Gamma_1^{(t)}(\mathbf{Q}, \boldsymbol{\theta})$ is given as

$$\begin{aligned}\Gamma_1^{(t)}(\mathbf{Q}, \boldsymbol{\theta}) &= -\epsilon^* R_1(\mathbf{Q}, \boldsymbol{\theta}) - (1 - \epsilon^*) R_2(\mathbf{Q}, \boldsymbol{\theta}) - \frac{1}{t} \log(\det \mathbf{Q}) - \frac{1}{t} \log(-\text{Tr}(\mathbf{Q}) + P_{\max}) \\ &\quad - \frac{1}{t} \sum_{n=1}^N \log(-\theta_n + 2\pi) - \frac{1}{t} \sum_{n=1}^N \log(\theta_n),\end{aligned}\quad (28)$$

and $-\frac{1}{t} \log(-x)$ is the logarithmic barrier function for the inequality constraints.

It is obvious that Problem (P2.3^{*}) is an approximation of Problem (P2.3), in which $t > 0$ is a parameter to set the accuracy of approximation, and the approximation increases as the t

increases [18]. It is worth pointing that when t is large, Problem (P2.3*) is complex to optimize by descent method due to the fact that the gradient of Problem (P2.3*) varies rapidly near the boundary of \mathcal{Q} . Therefore, we solve a sequence of Problem (P2.3*) for a sequence of increasing t , and the optimal point of previous Problem (P2.3*) is used as the starting point of next Problem (P2.3*) [18].

For Problem (P2.3*), we perform the gradient descent method to compute the optimal solution $\{\mathbf{Q}^{(t)}, \boldsymbol{\theta}^{(t)}\}$, where the descent direction $\{\Delta\mathbf{Q}, \Delta\boldsymbol{\theta}\}$ and the step size k are obtained as follows.

- **Descent Direction:** The descent direction $\{\Delta\mathbf{Q}, \Delta\boldsymbol{\theta}\}$ is the negative gradient of $\Gamma_1^{(t)}(\mathbf{Q}, \boldsymbol{\theta})$, i.e.,

$$\begin{aligned} \Delta\mathbf{Q} = & \epsilon^* \frac{\mathbf{H}^H \Phi^H \mathbf{h}_1 \mathbf{h}_1^H \Phi \mathbf{H}}{1 + \mathbf{h}_1^H \Phi \mathbf{H} \mathbf{Q} \mathbf{H}^H \Phi^H \mathbf{h}_1} + (1 - \epsilon^*) \frac{\mathbf{H}^H \Phi^H \mathbf{h}_2 \mathbf{h}_2^H \Phi \mathbf{H}}{1 + \mathbf{h}_2^H \Phi \mathbf{H} \mathbf{Q} \mathbf{H}^H \Phi^H \mathbf{h}_2} \\ & + \frac{\mathbf{I}}{t(\text{Tr}(\mathbf{Q}) - P_{\max})} + \frac{\mathbf{Q}^{-1}}{t}, \end{aligned} \quad (29)$$

$$\begin{aligned} \Delta\boldsymbol{\theta} = & \epsilon^* \frac{\Delta_1 \mathbf{H} \mathbf{Q} \mathbf{H}^H \Delta_1^H \boldsymbol{\varphi}}{1 + \mathbf{h}_1^H \Phi \mathbf{H} \mathbf{Q} \mathbf{H}^H \Phi^H \mathbf{h}_1} + (1 - \epsilon^*) \frac{\Delta_2 \mathbf{H} \mathbf{Q} \mathbf{H}^H \Delta_2^H \boldsymbol{\varphi}}{1 + \mathbf{h}_2^H \Phi \mathbf{H} \mathbf{Q} \mathbf{H}^H \Phi^H \mathbf{h}_2} \\ & - \boldsymbol{\nu}_1 + \boldsymbol{\nu}_2, \end{aligned} \quad (30)$$

$$\text{where } \boldsymbol{\nu}_1 = \left[\frac{1}{(2\pi - \theta_1)t}, \dots, \frac{1}{(2\pi - \theta_N)t} \right]^T, \quad \boldsymbol{\nu}_2 = \left[\frac{1}{\theta_1 t}, \dots, \frac{1}{\theta_N t} \right]^T.$$

- **Step Size:** Backtracking line search [18] is used to determine the step size l : first starts with $l = 1$ and then reduces l by $l := l\eta$, with $0 < \eta < 1$, until the stopping condition

$$\Gamma_1^{(t)}(\mathbf{Q} + l\Delta\mathbf{Q}, \boldsymbol{\theta} + l\Delta\boldsymbol{\theta}) < \Gamma_1^{(t)}(\mathbf{Q}, \boldsymbol{\theta}) - \alpha l (\|\Delta\mathbf{Q}\|_{m_2}^2 + \|\Delta\boldsymbol{\theta}\|^2) \quad (31)$$

satisfies, where $0 < \alpha < 0.5$ presents the fraction of the decrease in $\Gamma_1^{(t)}$ predicted by linear extrapolation that we set.

Overall Algorithm: Based on above discussion, we can compute the optimal solution $\{\mathbf{Q}_{\epsilon^*}, \boldsymbol{\theta}_{\epsilon^*}\}$ for Problem (P1.3) by two-level iterations, and the detailed algorithm is summarized in Algorithm 1. For the inner iteration, we compute $\{\mathbf{Q}^{(t)}, \boldsymbol{\theta}^{(t)}\}$ by gradient descent method. For the outer iteration, we increase the value of t , and the obtained $\{\mathbf{Q}^{(t)}, \boldsymbol{\theta}^{(t)}\}$ from the previous inner iteration is used as the starting point for the next inner iteration.

IV. OPTIMAL SOLUTION FOR THE CASE OF $K > 2$

The previous section only discusses the covariance matrix and phase shifts for a special situation, i.e., $K = 2$. For most practical situations, the number of MUs is greater than 2. In this

Algorithm 1 Compute the solution of Problem (P2.3) \mathbf{Q}_{ϵ^*} and $\boldsymbol{\theta}_{\epsilon^*}$

Input: $\mathbf{h}_1, \mathbf{h}_2, \mathbf{H}, P_{\max}, l_0, \rho > 0, 0 < \eta < 1$, and the error tolerances $\delta_1 > 0$ and $\delta_2 > 0$.

Output: $(\mathbf{Q}_{\epsilon^*}, \boldsymbol{\theta}_{\epsilon^*})$.

```

1: Initialize  $(\mathbf{Q}_{t_i}, \boldsymbol{\theta}_{t_i})$  and  $(\mathbf{Q}_j, \boldsymbol{\theta}_j)$  respectively represent the output of the  $i$ -th outer iteration
   and the input of the  $j$ -th inner iteration.
2: while  $\frac{1}{t_{i-1}} > \delta_1$  do
3:   Let  $t_i = \rho t_{i-1}$ .
4:   Initialize  $\mathbf{Q}_1 = \mathbf{Q}_{t_{i-1}}$  and  $\boldsymbol{\theta}_1 = \boldsymbol{\theta}_{t_{i-1}}$ .
5:   while  $\left| \Gamma_1^{(t_i)}(\mathbf{Q}_j, \boldsymbol{\theta}_j) - \Gamma_1^{(t_i)}(\mathbf{Q}_{j-1}, \boldsymbol{\theta}_{j-1}) \right| > \delta_2$  do
6:     Compute  $\Delta \mathbf{Q}_{j+1}$  and  $\Delta \boldsymbol{\theta}_{j+1}$  by (29) and (30), respectively.
7:     Initialize  $l_1 = l_0$ 
8:     while Condition (31) does not satisfy do
9:       Let  $l_i := l_{i-1}\eta$ .
10:      end while
11:      Let  $\mathbf{Q}_{j+1} = \mathbf{Q}_j + l_i \Delta \mathbf{Q}_{j+1}$  and  $\boldsymbol{\theta}_{j+1} = \boldsymbol{\theta}_j + l_i \Delta \boldsymbol{\theta}_{j+1}$ .
12:      end while
13:      Let  $\mathbf{Q}_{t_i} = \mathbf{Q}_{j+1}$  and  $\boldsymbol{\theta}_{t_i} = \boldsymbol{\theta}_{j+1}$ .
14:    end while
15:  Let  $(\mathbf{Q}_{\epsilon^*}, \boldsymbol{\theta}_{\epsilon^*}) = (\mathbf{Q}_{t_i}, \boldsymbol{\theta}_{t_i})$ .

```

section, we consider Problem (P1) for $K > 2$. First, the necessary condition of optimal solution for $K > 2$ is given as follows.

A. Necessary Condition of Optimal Solution for $K > 2$

It is obvious that objective function (5) in Problem (P1) is non-differentiable, and thus we cannot directly obtain the necessary condition of optimal solution for Problem (P1) by the KKT condition. However, it can be observed that Problem (P1) can be reformulated as

$$(P3) \quad \max_{\mathbf{Q}, \boldsymbol{\theta}, T} \quad T \quad (32)$$

$$\text{s.t. } T \leq \mathbf{h}_k^H \Phi \mathbf{H} \mathbf{Q} \mathbf{H}^H \Phi^H \mathbf{h}_k, k = 1, \dots, K \quad (33)$$

$$(6), (7), (8),$$

and Problems (P1) and (P3) own the same optimal solution $\{\mathbf{Q}_{\epsilon^*}, \boldsymbol{\theta}_{\epsilon^*}\}$, while Problem (P3) is differentiable. Since Problem (P3) is differentiable and non-convex, we can characterize the necessary condition of the optimal solution of Problem (P3) by the KKT condition. By taking

the derivative of Lagrangian of Problem (P3), i.e.,

$$\begin{aligned} L = & -T + \sum_{k=1}^K \lambda_{k,0} (T - \mathbf{h}_k^H \Phi \mathbf{H} \mathbf{Q} \mathbf{H}^H \Phi^H \mathbf{h}_k) + \mu (\text{Tr}(\mathbf{Q}) - P_{\max}) \\ & - \text{Tr}(\Psi \mathbf{Q}) + \sum_{n=1}^N \lambda_{n,1} (\theta_n - 2\pi) - \sum_{n=1}^N \lambda_{n,2} \theta_n, \end{aligned} \quad (34)$$

we obtain the necessary condition of optimal solution for Problem (P3):

$$-1 + \sum_{k=1}^K \lambda_{k,0} = 0, \quad (35)$$

$$\sum_{k=1}^K \lambda_{k,0} \mathbf{H}^H \Phi^H \mathbf{h}_k \mathbf{h}_k^H \Phi \mathbf{H} + \mu \mathbf{I} - \Psi = \mathbf{0}, \quad (36)$$

$$\sum_{k=1}^K \lambda_{k,0} \Delta_k \mathbf{H} \mathbf{Q} \mathbf{H}^H \Delta_k^H \varphi + \boldsymbol{\lambda}_1 - \boldsymbol{\lambda}_2 = \mathbf{0}, \quad (37)$$

$$\text{Tr}(\mathbf{Q}) \leq P_{\max}, \quad \mathbf{Q} \succeq \mathbf{0}, \quad \mu \geq 0, \quad \Psi \succeq \mathbf{0}, \quad (38)$$

$$\mu (\text{Tr}(\mathbf{Q}) - P_{\max}) = 0, \quad \Psi \mathbf{Q} = \mathbf{0}, \quad (39)$$

$$\lambda_{n,1} (\theta_n - 2\pi) = 0, \quad -\lambda_{n,2} \theta_n = 0, \quad 0 \leq \theta_n \leq 2\pi, \quad \lambda_{n,1} \geq 0, \quad \lambda_{n,2} \geq 0, \quad n = 1, \dots, N, \quad (40)$$

$$T \leq \mathbf{h}_k^H \Phi \mathbf{H} \mathbf{Q} \mathbf{H}^H \Phi^H \mathbf{h}_k, \quad \lambda_{k,0} (T - \mathbf{h}_k^H \Phi \mathbf{H} \mathbf{Q} \mathbf{H}^H \Phi^H \mathbf{h}_k) = 0, \quad k = 1, \dots, K. \quad (41)$$

We can adopt a brute-force search over $\{\mathbf{Q}, \boldsymbol{\theta}, T\}$, which satisfies the necessary condition (35)-(41) to obtain the optimal solution $\{\mathbf{Q}^*, \boldsymbol{\theta}^*\}$ for Problem (P1). However, the time complexity of implementing brute-force search for (35)-(41) is very high. Therefore, we propose two algorithms to approach the optimal solution $\{\mathbf{Q}^*, \boldsymbol{\theta}^*\}$ in the next subsections.

B. Subgradient Descent Method

Since Problem (P1) is not differentiable, the gradients are non-existent for some $\{\mathbf{Q}, \boldsymbol{\theta}\}$. Thus, the subgradient descent method is considered to approach the optimal solution for Problem (P1). The detail steps are given as follows.

First, due to the fact that Problem (P1) owns the inequality constraints, we rewrite Problem (P1), making the inequality constraints implicit in the objective function:

$$(\text{P1}^*) \quad \min \Gamma_2^{(t)} (\mathbf{Q}, \boldsymbol{\theta}), \quad (42)$$

where $\Gamma_2^{(t)}(\mathbf{Q}, \boldsymbol{\theta})$ is given as

$$\begin{aligned}\Gamma_2^{(t)}(\mathbf{Q}, \boldsymbol{\theta}) = & -\max_{k=1, \dots, K} \log (1 + \mathbf{h}_k^H \Phi \mathbf{H} \mathbf{Q} \mathbf{H}^H \Phi^H \mathbf{h}_k) - \frac{1}{t} \log (-\text{Tr}(\mathbf{Q}) + P_{\max}) \\ & - \frac{1}{t} \log (\det \mathbf{Q}) - \frac{1}{t} \sum_{n=1}^N \log(-\theta_n + 2\pi) - \frac{1}{t} \sum_{n=1}^N \log (\theta_n).\end{aligned}\quad (43)$$

Similar to Algorithm 1, we solve a sequence of Problem (P1*) for sequence of increasing t , and the optimal point of previous Problem (P1*) is used as the starting point of the next Problem (P1*).

We adopt the gradient descent method to compute the optimal solution $\{\mathbf{Q}^{(t)}, \boldsymbol{\theta}^{(t)}\}$ for Problem (P1*) with the fixed t . Thus, we need to obtain the descent direction and step size.

1) *Descent Direction*: It is different from Problem (P2.3*) that Problem (P1*) is non-differentiable everywhere. Thus, we set the subgradient of $\Gamma_2^{(t)}(\mathbf{Q}, \boldsymbol{\theta})$ as the descent direction $(\Delta \mathbf{Q}, \Delta \boldsymbol{\theta})$.

Proposition 4.1: For given in $\{\mathbf{Q}, \boldsymbol{\theta}\}$, the subgradients of $\Gamma_2^{(t)}(\mathbf{Q}, \boldsymbol{\theta})$ are given as

$$\Delta \mathbf{Q} = \frac{\mathbf{H}^H \Phi^H \mathbf{h}_{k^*} \mathbf{h}_{k^*}^H \Phi \mathbf{H}}{1 + \mathbf{h}_{k^*}^H \Phi \mathbf{H} \mathbf{Q} \mathbf{H}^H \Phi^H \mathbf{h}_{k^*}} + \frac{\mathbf{I}}{t(\text{Tr}(\mathbf{Q}) - P_{\max})} + \frac{\mathbf{Q}^{-1}}{t}, \quad (44)$$

$$\Delta \boldsymbol{\theta} = \frac{\Delta_{k^*} \mathbf{H} \mathbf{Q} \mathbf{H}^H \Delta_{k^*}^H \boldsymbol{\varphi}}{1 + \mathbf{h}_{k^*}^H \Phi \mathbf{H} \mathbf{Q} \mathbf{H}^H \Phi^H \mathbf{h}_{k^*}} - \boldsymbol{\nu}_1 + \boldsymbol{\nu}_2, \quad (45)$$

where k^* are elements of the set \mathbf{k}^* , which is given by

$$\mathbf{k}^* = \left\{ k^* : k^* = \arg \max_{k=1, \dots, K} \log (1 + \mathbf{h}_k^H \Phi \mathbf{H} \mathbf{Q} \mathbf{H}^H \Phi^H \mathbf{h}_k) \right\}. \quad (46)$$

Proof: Based on [18], it is obtained that for pointwise maximum $\Gamma_2^{(t)}(\mathbf{Q}, \boldsymbol{\theta})$, the subgradients of that are the negative gradients of

$$\begin{aligned}-\log (1 + \mathbf{h}_{k^*}^H \Phi \mathbf{H} \mathbf{Q} \mathbf{H}^H \Phi^H \mathbf{h}_{k^*}) - \frac{1}{t} \log (-\text{Tr}(\mathbf{Q}) + P_{\max}) \\ - \frac{1}{t} \log (\det \mathbf{Q}) - \frac{1}{t} \sum_{n=1}^N \log(-\theta_n + 2\pi) - \frac{1}{t} \sum_{n=1}^N \log (\theta_n),\end{aligned}\quad (47)$$

where k^* are elements of the set \mathbf{k}^* given as (46). By taking the derivative of the function (47), the negative gradients are obtained as (44) and (45), which completes this proof. \blacksquare

Remark 4.1: If the set \mathbf{k}^* only owns one element for given in $\{\mathbf{Q}, \boldsymbol{\theta}\}$, the function $\Gamma_2^{(t)}(\mathbf{Q}, \boldsymbol{\theta})$ is differentiable at \mathbf{Q} and $\boldsymbol{\theta}$, which implies that the descent direction is the negative gradient of $\Gamma_2^{(t)}(\mathbf{Q}, \boldsymbol{\theta})$. If the set \mathbf{k}^* owns multiple elements, the function $\Gamma_2^{(t)}(\mathbf{Q}, \boldsymbol{\theta})$ is non-differentiable, and the descent direction can be any subgradient of $\Gamma_2^{(t)}(\mathbf{Q}, \boldsymbol{\theta})$ at \mathbf{Q} and $\boldsymbol{\theta}$.

2) *Step Size*: We also adopt the backtracking line search to determine the step size k . First starts with $k = 1$ and then reduces k by $k := k\eta$, with $0 < \eta < 1$, until the stopping condition

$$\Gamma_2^{(t)}(\mathbf{Q} + k\Delta\mathbf{Q}, \boldsymbol{\theta} + k\Delta\boldsymbol{\theta}) < \Gamma_2^{(t)}(\mathbf{Q}, \boldsymbol{\theta}) - \alpha k (\|\Delta\mathbf{Q}\|_{m_2}^2 + \|\Delta\boldsymbol{\theta}\|^2) \quad (48)$$

satisfies.

C. Gradient Descent Method

Since Problems (P1) and (P3) own the same optimal solution, we compute the optimal solution $(\mathbf{Q}^*, \boldsymbol{\theta}^*, T^*)$ for Problem (P3) to indirectly obtain that for Problem (P1). Due to the fact that Problem (3) is an inequality constrained optimization problem and continuously differentiable, it is different from Problem (P1) that we can obtain the gradient descent for Problem (P3). Thus, Problem (P3) can be solved by Algorithm 1. Here, we only point out the difference, i.e., the descent direction.

In order to obtain the descent direction for Problem (P3), we first need to reformulate the inequality constrained Problem (P3) as the unconstrained problem (P3*):

$$(\text{P3}^*) \quad \min \Gamma_3^{(t)}(\mathbf{Q}, \boldsymbol{\theta}), \quad (49)$$

where $\Gamma_3^{(t)}(\mathbf{Q}, \boldsymbol{\theta}, T)$ is given as

$$\begin{aligned} \Gamma_3^{(t)}(\mathbf{Q}, \boldsymbol{\theta}, T) = & -T - \frac{1}{t} \sum_{k=1}^K \log(-T + \mathbf{h}_k^H \Phi \mathbf{H} \mathbf{Q} \mathbf{H}^H \Phi^H \mathbf{h}_k) - \frac{1}{t} \log(-\text{Tr}(\mathbf{Q}) + P_{\max}) \\ & - \frac{1}{t} \log(\det \mathbf{Q}) - \frac{1}{t} \sum_{n=1}^N \log(-\theta_n + 2\pi) - \frac{1}{t} \sum_{n=1}^N \log(\theta_n). \end{aligned} \quad (50)$$

Then, by taking the derivative $\Gamma_3^{(t)}(\mathbf{Q}, \boldsymbol{\theta}, T)$ at \mathbf{Q} , $\boldsymbol{\theta}$, and T , we obtain the descent direction:

$$\Delta\mathbf{Q} = \frac{1}{t} \sum_{k=1}^K \frac{\mathbf{H}^H \Phi^H \mathbf{h}_1 \mathbf{h}_1^H \Phi \mathbf{H}}{-T + \mathbf{h}_k^H \Phi \mathbf{H} \mathbf{Q} \mathbf{H}^H \Phi^H \mathbf{h}_k} + \frac{\mathbf{I}}{t(\text{Tr}(\mathbf{Q}) - P_{\max})} + \frac{\mathbf{Q}^{-1}}{t}, \quad (51)$$

$$\Delta\boldsymbol{\theta} = \frac{1}{t} \sum_{k=1}^K \frac{\Delta_1 \mathbf{H} \mathbf{Q} \mathbf{H}^H \Delta_1^H \boldsymbol{\varphi}}{-T + \mathbf{h}_k^H \Phi \mathbf{H} \mathbf{Q} \mathbf{H}^H \Phi^H \mathbf{h}_k} - \boldsymbol{\nu}_1 + \boldsymbol{\nu}_2, \quad (52)$$

$$\Delta T = 1 - \frac{1}{t} \sum_{k=1}^K \frac{1}{-T + \mathbf{h}_k^H \Phi \mathbf{H} \mathbf{Q} \mathbf{H}^H \Phi^H \mathbf{h}_k}. \quad (53)$$

After obtaining the descent direction, the optimal solution $\{\mathbf{Q}^*, \boldsymbol{\theta}^*, T^*\}$ can be computed by Algorithm 1.

V. ASYMPTOTIC ANALYSIS

In the previous two sections, the capacity of multicast transmission assisted by RIS was maximized via the numerical algorithms, which lose some intuition for the performance of RIS in multicast transmission. Thus, this section analyzes the order growth of C^* in some special scenarios, i.e., the numbers of reflecting elements, BS antennas, and MUs go to infinity. In this section, we consider independent and identically distributed (i.i.d.) Ralyleigh fading with \mathbf{h}_k^H , and \mathbf{H} is also Ralyleigh fading, i.e., $h_{k,n}$ and $H_{n,m}$ are i.i.d. complex Gaussian distribution with $\mathcal{CN}(0, 1)$.

A. Fixed MUs, Increasing Antennas and reflecting elements

First, we consider the scenarios where the numbers of reflecting elements and BS antennas go to infinity.

Proposition 5.1: If K is fixed, the order growth of C^* is given as follows.

- When N is fixed and M goes to infinity, C^* grows at the following rate

$$C^* \approx O(\log M). \quad (54)$$

- When M is fixed and N goes to infinity, C^* grows at the following rate

$$C^* \approx O(\log N). \quad (55)$$

- When N and M both go to infinity, C^* grows at the following rate

$$C^* \approx O(\log NM). \quad (56)$$

Proof: Please see Appendix B ■

From Proposition 5.1, we obtain that C^* goes to infinity, as the numbers of reflecting elements or BS antennas go to infinity, and C^* is logarithmic growth, which conforms intuition.

B. Fixed Antennas and reflecting elements, Increasing MUs

Then, we consider the scenarios that the number of the MUs K goes to infinity. It is obvious that when N and M are fixed, $\min_{k=1, \dots, K} \{\|\mathbf{h}_k^H\|\} \rightarrow 0$, as $K \rightarrow \infty$, which implies that there

must be at least one link between the RIS and MU being completely cut off, and it follows $C^* \rightarrow 0$. Here, we focus on studying the rate of $C^* \rightarrow 0$.

Proposition 5.2: When N and M both are fixed, and K goes to infinity, C^* decrease to 0 at the following rate

$$C^* \approx O\left(\frac{1}{K^{1/NM}}\right) \quad (57)$$

Proof: First, as $h_{k,n} \sim \mathcal{CN}(0, 1)$, $H_{n,m} \sim \mathcal{CN}(0, 1)$ and $|\phi_n| = 1$, we obtain $h_{k,n}\phi_n H_{n,m} \sim \mathcal{CN}(0, 1)$, and it follows $\Psi_{m,k} = \sum_{n=1}^N h_{k,n}\phi_n H_{n,m} \sim \mathcal{CN}(0, N)$. From (84) and $\Psi_{m,k} \sim \mathcal{CN}(0, N)$, it is easy to obtain that the $\|\mathbf{h}_k^H \Phi \mathbf{H}\|^2$ is non-central chi-square distribution with $2M$ degrees of freedom and its mean is NM .

Then, from [15], it is concluded that the minimum of K non-central chi-squared random variables $\|\mathbf{h}_k^H \Phi \mathbf{H}\|^2$, i.e., $\min_{k=1, \dots, K} \{\|\mathbf{h}_k^H \Phi \mathbf{H}\|^2\}$, can be scaled as $K^{-1/NM}$.

Please notice that C^* is upper bounded by the minimum of the point-to-point capacity of RIS system:

$$C^* \leq \log \left(1 + P_{\max} \min_{k=1, \dots, K} \|\mathbf{h}_k^H \Phi \mathbf{H}\|^2 \right) \quad (58)$$

$$\approx \log \left(1 + \frac{P_{\max}}{K^{1/NM}} \right) \quad (59)$$

$$\approx \frac{P_{\max}}{K^{1/NM}}, \quad (60)$$

which is $O\left(\frac{1}{K^{1/NM}}\right)$, and then C^* is lower bounded by spatially white rate [15]:

$$C^* \geq \log \left(1 + \frac{P_{\max}}{N} \min_{k=1, \dots, K} \|\mathbf{h}_k^H \Phi \mathbf{H}\|^2 \right) \quad (61)$$

$$\approx \frac{P_{\max}}{NK^{1/NM}}, \quad (62)$$

which is also $O\left(\frac{1}{K^{1/NM}}\right)$. ■

C. Increasing MUs, Antennas and reflecting elements

From Propositions 5.1 and 5.2, it is easy to see that when N and M go to the infinity, C^* goes to infinity; however when K goes to the infinity, C^* goes to zero. **It leads us focusing on the behavior of the order growth of C^* , as N , M , and K simultaneously increasing to infinity.**

Proposition 5.3: When M and K goes to infinity simultaneously at the ratio $0 < \frac{M}{K} < \infty$, we obtain:

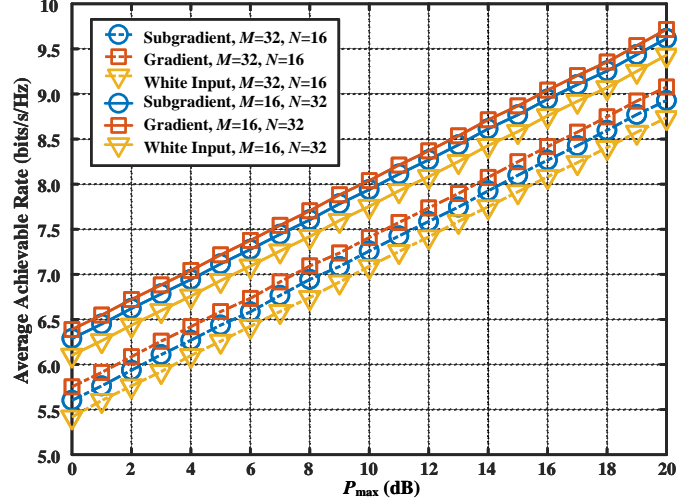


Fig. 2: Average achievable rates versus the power budget P_{\max} , where $K = 16$.

- if N is fixed, then

$$\mathbb{E} \{C^*\} \approx O(1). \quad (63)$$

- if N goes to infinity, then

$$O(1) \leq \mathbb{E} \{C^*\} \leq O(\log(N^2)). \quad (64)$$

Proof: Please see Appendix C. ■

VI. NUMERICAL RESULTS

This section shows the numerical results of achievable rates for RIS multicast channel under the different descent methods. As a comparison, we also compute the achievable rate under the spatially white input covariance $\mathbf{Q} = \frac{P_{\max}}{M} \mathbf{I}$ and zero phase shifts $\boldsymbol{\theta} = \mathbf{0}$. Each element of \mathbf{H} and \mathbf{h}_k^H is randomly generated with complex Gaussian distribution $\mathcal{CN}(0, 1)$. Under the same conditions, we compute the achievable rates for 10000 times, and present the average of that.

Fig. 2 shows the average achievable rate as a function of P_{\max} for RIS multicast transmission under the subgradient and gradient descent methods, as well as spatially white input, where the numbers of reflecting elements are set as $N = 16, 32$, respectively, the number of antennas are also set as $M = 16, 32$, respectively, and the number of users is $K = 16$. From the curves in Fig. 2, it is observed that the average achievable rates increase as P_{\max} increases. The average achievable rates under the gradient descent method are around 0.15 bits/s/Hz and 0.2 bits/s/Hz

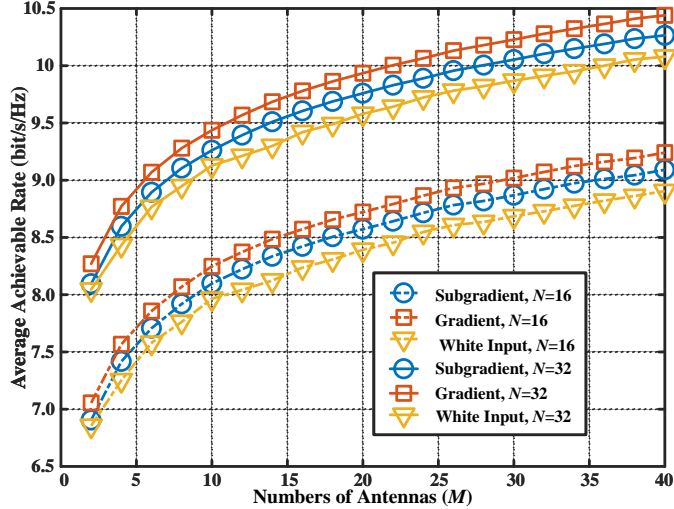


Fig. 3: Average achievable rates versus the number of antennas M , where $P = 20(\text{dB})$, $K = 16$.

better than that under the subgradient decent method in $M = 32$, $N = 16$ case and in $M = 16$, $N = 32$ case, respectively. The two methods are both greater than spatially white input, and the average achievable rate in $M = 16$, $N = 32$ case is higher than that in $M = 32$, $N = 16$ case.

Fig. 3 presents the average achievable rates versus the numbers of antennas M , where the numbers of reflecting elements are set as $N = 16$, 32, respectively, the power budget is set as $P_{\max} = 20(\text{dB})$, and the number of users is set as $K = 16$. From Fig. 3, we observe that the average achievable rates are logarithmic growth as the increasing of the number of reflecting elements N . The two methods are both greater than spatially white input. The gaps between the gradient and subgradient descent methods steadily increase to about 0.15 bits/s/Hz and 0.17 bits/s/Hz in $N = 16$ and $N = 32$ cases, respectively, which implies that the gradient descent method owns better performance than subgradient descent method.

Fig. 4 plots the average achievable rates versus the numbers of reflecting elements N , where the numbers of antennas are set as $M = 16$, 32, respectively, the power budget is set as $\frac{P_{\max}}{\sigma^2} = 20$ (dB), and the number of MUs is set as $K = 16$. From the curves in Fig. 4, it is observed that the average achievable rates are also logarithmic growth as N increases. The gaps between the gradient and subgradient descent methods increase to about 0.1 bits/s/Hz in both $N = 16$ and $N = 32$ cases, and the gaps between the subgradient descent method and spatially white input almost are constants 0.18 bits/s/Hz and 0.19 bits/s/Hz in $N = 16$ and $N = 32$ cases, respectively.

Fig. 5 represents the average achievable rate versus the numbers of antennas M and reflecting

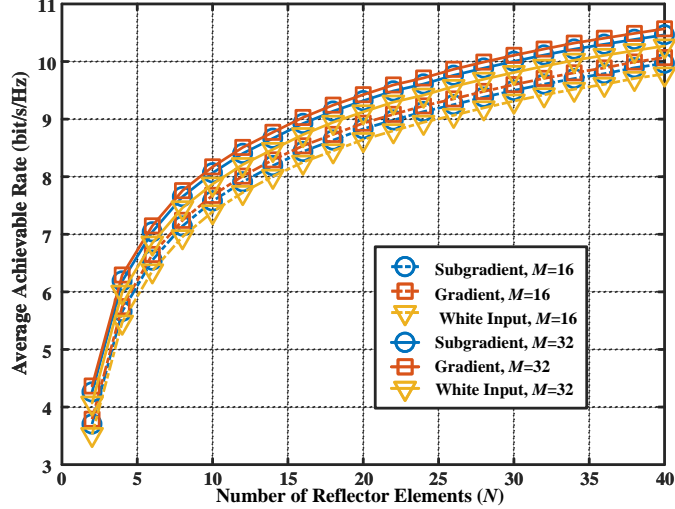


Fig. 4: Average achievable rates versus the number of reflecting elements N , where $P = 20$ (dB), $K = 16$.

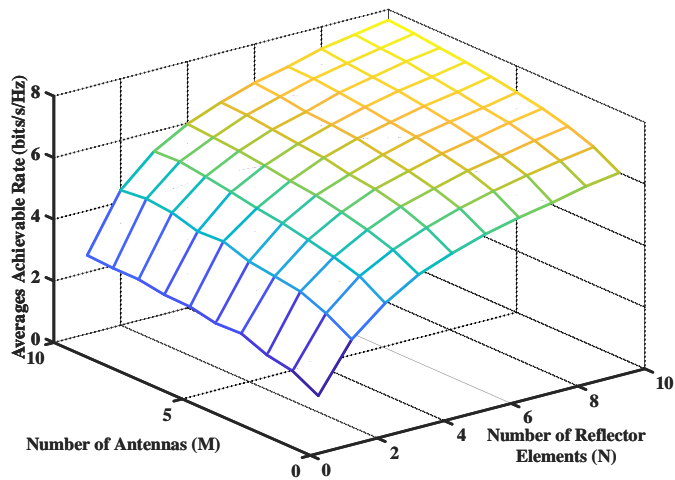


Fig. 5: Average achievable rate versus the numbers of antennas M and reflecting elements N with gradient descent method, where $P = 20$ (dB), $K = 4$.

elements N under the gradient descent method, where $P = 20$ (dB), and $K = 4$. From Fig. 5, it can be observed that the average achievable rates are logarithmic growth as N and M increase. Please notice that the growth rate of achievable rate with N is obviously higher than that with M , which implies that increasing the number of reflecting elements can obtain the better performance than increasing the number of antennas.

Fig. 6 shows the relationship between the average achievable rates and the numbers of MUs K , where the numbers of reflecting elements and antennas are set as $N = 4$ and $M = 4$,

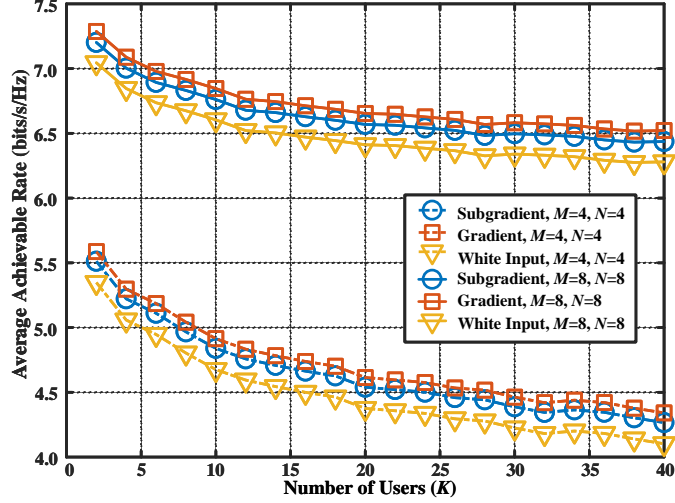


Fig. 6: Average achievable rates versus the number of MUs K .

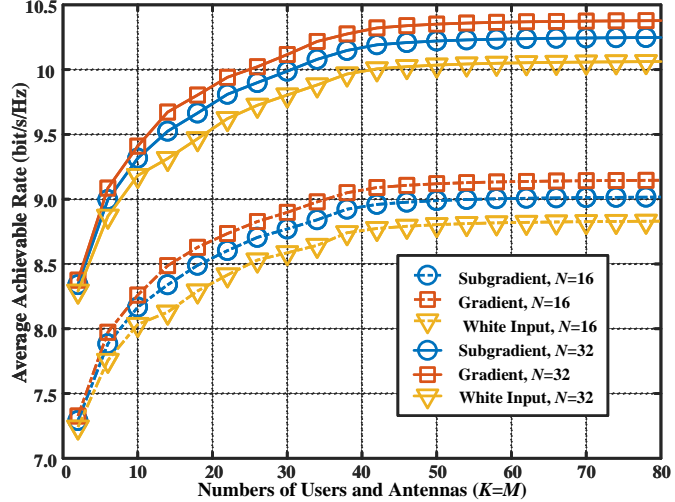


Fig. 7: Average achievable rate versus the equal number of MUs K , where $P = 20$ (dB).

respectively, and the power budget is set as $P_{\max} = 20$ (dB). From Fig. 6, we can observe that the average achievable rates decrease as increases K at the rate $O\left(\frac{1}{K^{1/NM}}\right)$. In $M, N = 4$ case, the average achievable rate decreases by around 2.5 bits/s/Hz, and in $M, N = 8$ case, that decreased by around 1.5 bits/s/Hz, which implies the reduction rate of the average achievable rates decreases as M and N increase.

Fig. 7 shows the average achievable rates versus the equal numbers of MUs K and antennas M (i.e., $\frac{K}{M} = 1$), where the numbers of reflecting elements are set as $N = 16, 32$, respectively, and the power budget is set as $P_{\max} = 20$ (dB). From Fig. 7, it can be observed that the

average achievable rates under gradient descent method are logarithmic growth as K first, and then remain constants around 9 bits/s/Hz and 10.5 bits/s/Hz for $N = 16$ and $N = 32$ cases, respectively. The subgradient descent method is about 0.15 bits/s/Hz lower than gradient descent method, and the gaps between the subgradient descent method and spatially white input are 0.19 bits/s/Hz for both the two cases.

VII. CONCLUSION

In this paper, we considered a multicast transmission that a multiple antenna BS sends the common message to multiple single-antenna MUs, where an RIS is deployed as a AF no-power relay to assist this transmission. First, we formulated a capacity maximization problem for two MUs scenario, and optimized covariance matrix and phase shifts by KKT conditions and a proposed numerical algorithm. Then, we generalized this problem to multiple MUs scenario, and adopted the subgradient and gradient descent methods to solve it. Last, we analyze the order growth for the maximum capacity of the multicast transmission assisted by RIS when the numbers of reflecting elements, BS antennas, and MUs go to infinity .

APPENDIX A

PROOF OF PROPOSITION 3.1

The main idea of this proof is to adopt the KKT conditions for obtaining the optimal solution for Problem (P2.1).

First, we can derive that $\|\mathbf{h}_2^H \Phi \mathbf{H}\|^2$ can be rewritten as

$$\begin{aligned} & \|\mathbf{h}_2^H \Phi \mathbf{H}\|^2 \\ &= \left[\sum_{n=1}^N h_{2,n} \phi_n H_{n,1}, \dots, \sum_{n=1}^N h_{2,n} \phi_n H_{n,M} \right] \left[\sum_{n=1}^N \bar{h}_{2,n} \bar{\phi}_n \bar{H}_{n,1}, \dots, \sum_{n=1}^N \bar{h}_{2,n} \bar{\phi}_n \bar{H}_{n,M} \right]^H \end{aligned} \quad (65)$$

$$= \sum_{m=1}^M \left| \sum_{n=1}^N h_{2,n} \phi_n H_{n,m} \right|^2 \quad (66)$$

$$= \sum_{m=1}^M \sum_{i=1}^N \sum_{j=1}^N a_{h_{2,i}} e^{j\theta_{h_{2,i}}} a_{h_{2,j}} e^{-j\theta_{h_{2,j}}} e^{j\theta_i} e^{-j\theta_i} a_{H_{i,m}} e^{j\theta_{H_{i,m}}} a_{H_{j,m}} e^{-j\theta_{H_{j,m}}} \quad (67)$$

$$= \sum_{m=1}^M \sum_{i=1}^N \sum_{j=1}^N a_{h_{2,i}} a_{h_{2,j}} a_{H_{i,m}} a_{H_{j,m}} e^{j(\theta_{h_{2,i}} - \theta_{h_{2,j}} + \theta_i - \theta_j + \theta_{H_{i,m}} - \theta_{H_{j,m}})} \quad (68)$$

$$\begin{aligned} &= \sum_{m=1}^M \sum_{i=1}^N \sum_{j=i+1}^N a_{h_{2,i}} a_{h_{2,j}} a_{H_{i,m}} a_{H_{j,m}} 2 \cos(\theta_{h_{2,i}} - \theta_{h_{2,j}} + \theta_i - \theta_j + \theta_{H_{i,m}} - \theta_{H_{j,m}}) \\ &+ \sum_{m=1}^M \sum_{n=1}^N |a_{h_{2,n}}|^2 |a_{H_{n,m}}|^2, \end{aligned} \quad (69)$$

where

- (67) is due to $h_{2,n} = a_{h_{2,n}} e^{j\theta_{h_{2,n}}}$ and $H_{n,m} = a_{H_{n,m}} e^{j\theta_{H_{n,m}}}$;
- (68) is due to the combination of (67);
- (69) is due to

$$\begin{aligned} & e^{j(\theta_{h_{2,i}} - \theta_{h_{2,j}} + \theta_i - \theta_j + \theta_{H_{i,m}} - \theta_{H_{j,m}})} + e^{j(\theta_{h_{2,j}} - \theta_{h_{2,i}} + \theta_j - \theta_i + \theta_{H_{j,m}} - \theta_{H_{i,m}})} \\ &= 2 \cos(\theta_{h_{2,i}} - \theta_{h_{2,j}} + \theta_i - \theta_j + \theta_{H_{i,m}} - \theta_{H_{j,m}}), \end{aligned} \quad (70)$$

and $\cos(\theta_{h_{2,i}} - \theta_{h_{2,j}} + \theta_i - \theta_j + \theta_{H_{i,m}} - \theta_{H_{j,m}}) = 1$ for $i = j$.

Then, from (69), we can observe that maximizing $\|\mathbf{h}_2^H \Phi \mathbf{H}\|^2$ is equivalent to

$$\max_{\theta: \theta_n \in [0, 2\pi], n=1, 2, \dots, N} \sum_{m=1}^M \sum_{i=1}^N \sum_{j=i+1}^N 2G_{i,j,m}^{(2)} \cos(\theta_i - \theta_j + \vartheta_{i,j,m}^{(2)}), \quad (71)$$

where $G_{i,j,m}^{(2)} = a_{h_{2,i}} a_{h_{2,j}} a_{H_{i,m}} a_{H_{j,m}}$ and $\vartheta_{i,j,m}^{(2)} = \theta_{h_{2,i}} - \theta_{h_{2,j}} + \theta_{H_{i,m}} - \theta_{H_{j,m}}$.

The Lagrangian of (71) is given as

$$L = - \sum_{m=1}^M \sum_{i=1}^N \sum_{j=i+1}^N 2G_{i,j,m}^{(2)} \cos \left(\theta_i - \theta_j + \vartheta_{i,j,m}^{(2)} \right) + \sum_{n=1}^N \lambda_{n,1} (\theta_n - 2\pi) - \sum_{n=1}^N \lambda_{n,2} \theta_n, \quad (72)$$

where $\lambda_{n,1}$ and $\lambda_{n,2}$, $n = 1, \dots, N$ are Lagrangian multipliers, which implies the KKT conditions of (71) is given as

$$\sum_{m=1}^M \sum_{j=1, j \neq i}^N 2G_{i,j,m}^{(2)} \sin \left(\theta_i - \theta_j + \vartheta_{i,j,m}^{(2)} \right) + \lambda_{i,1} - \lambda_{i,2} = 0, \quad i = 1, \dots, N \quad (73)$$

$$\lambda_{n,1} (\theta_n - 2\pi) = 0, \quad -\lambda_{n,2} \theta_n = 0, \quad n = 1, \dots, N \quad (74)$$

$$0 \leq \theta_n \leq 2\pi, \quad \lambda_{n,1} \geq 0, \quad \lambda_{n,2} \geq 0, \quad n = 1, \dots, N. \quad (75)$$

Based on [18], we know the KKT conditions (75) is necessary condition of the optimal solution for (71), i.e., Problem (P2.1), and thus (18) is derived, which completes the proof.

APPENDIX B

PROOF OF PROPOSITION 5.1

It is obvious that C^* is smaller than the capacity of the channel from BS to any UM, i.e.,

$$C^* \leq \max_{\theta} \log \left(1 + P_{\max} \left\| \mathbf{h}_k^H \Phi \mathbf{H} \right\|^2 \right), \quad (76)$$

which is also an upper bound for C^* . Form (3) and (2), we obtain

$$\mathbf{h}_k^H \Phi \mathbf{H} = [\Psi_1, \Psi_2, \dots, \Psi_{m,k}] \quad (77)$$

where $\Psi_{m,k} = \sum_{n=1}^N h_{k,n} \phi_n H_{n,m}$. It is obvious that

$$\mathbb{E} \{ |\Psi_{m,k}|^2 \} \quad (78)$$

$$= \mathbb{E} \left\{ \left| \sum_{n=1}^N h_{k,n} \phi_n H_{n,m} \right|^2 \right\} \quad (79)$$

$$= \sum_{n=1}^N \mathbb{E} \{ |h_{k,n} \phi_n H_{n,m}|^2 \} \quad (80)$$

$$= \sum_{n=1}^N \mathbb{E} \{ |h_{k,n}|^2 |H_{n,m}|^2 \} \quad (81)$$

$$= \sum_{n=1}^N \mathbb{E} \{ |h_{k,n}|^2 \} \mathbb{E} \{ |H_{n,m}|^2 \} + 2\mathbb{E}^2 \{ h_{k,n} H_{n,m} \} \quad (82)$$

$$= N, \quad (83)$$

where

- (80) is due to the fact that $\{h_{k,n} \phi_n H_{n,m}\}$ is i.i.d.;
- (81) is due to $|\phi_n|^2 = 1$.
- (83) is due to $\mathbb{E} \{ |h_{k,n}|^2 \} = 1$, $\mathbb{E} \{ |H_{n,m}|^2 \} = 1$, and $\mathbb{E} \{ h_{k,n} H_{n,m} \} = 0$.

Then, based on the law of large numbers and (83), it follows

$$\| \mathbf{h}_k^H \Phi \mathbf{H} \|^2 = \sum_{m=1}^M |\Psi_{m,k}|^2 \quad (84)$$

$$\rightarrow M \mathbb{E} \{ |\Psi_{m,k}|^2 \} \quad (85)$$

$$= MN, \quad (86)$$

a.s., as $M \rightarrow \infty$. Thus, C^* is upper bounded by

$$\log (1 + P_{\max} MN). \quad (87)$$

Next, from [15], it is obtained that C^* is lower bounded in

$$\max_{\theta} \log \left(1 + \frac{P_{\max}}{K^2} \| \mathbf{h}_k^H \Phi \mathbf{H} \|^2 \right). \quad (88)$$

By the same proof for the upper bound of C^* , the lower bound of that can be rewritten as

$$\begin{aligned} & \max_{\theta} \log \left(1 + \frac{P_{\max}}{K^2} \|\mathbf{h}_k^H \Phi \mathbf{H}\|^2 \right) \\ & \rightarrow \log \left(1 + P_{\max} \frac{MN}{K^2} \right), \end{aligned} \quad (89)$$

a.s., as $M \rightarrow \infty$.

From the upper and lower bounds (87) and (89), we obtain that

- When K and N are fixed and M goes to infinity, both the upper and lower bounds of C^* are $O(\log M)$, and it follows (54);
- When N and M go to infinity and K is fixed, both the upper and lower bounds of C^* are $O(\log NM)$, and it follows (56).

Last, the proof of (55) is similar to that of (54) and (56), and thus we only show its difference.

By the law of large number, we can obtain that as $N \rightarrow \infty$,

$$|\Psi_{m,k}|^2 = \sum_{n=1}^N \sum_{i=1}^N h_{k,n} \bar{h}_{k,i} \phi_n \bar{\phi}_i H_{n,m} \bar{H}_{i,m} \quad (90)$$

$$\rightarrow \sum_{n=1}^N \mathbb{E} \{ |h_{k,n}|^2 |\phi_n|^2 |H_{n,m}|^2 \} \quad (91)$$

$$= N, \quad (92)$$

a.s., where (91) is due to

$$\sum_{n=1}^N \sum_{i=1, i \neq n}^N h_{k,n} \bar{h}_{k,i} \phi_n \bar{\phi}_i H_{n,m} \bar{H}_{i,m} \quad (93)$$

$$= \sum_{n=1}^N \sum_{i=1, i \neq n}^N \mathbb{E} \{ h_{k,n} \bar{h}_{k,i} \phi_n \bar{\phi}_i H_{n,m} \bar{H}_{i,m} \} \quad (94)$$

$$= 0, \quad (95)$$

as $N \rightarrow \infty$. It follows $\|\mathbf{h}_k^H \Phi \mathbf{H}\|^2 = MN$, as $N \rightarrow \infty$. The other steps of this proof is same to the proof of (54) and (56), and thus is omitted.

APPENDIX C
PROOF OF PROPOSITION 5.3

We first show the lower bound of $\mathbb{E}\{C^*\}$. From the proof of Propositions 5.1, we obtain that the mean of $\|\mathbf{h}_k^H \Phi \mathbf{H}\|^2$ is NM and the variance of that is $2N^2M$. It follows that the mean and variance of $\frac{\|\mathbf{h}_k^H \Phi \mathbf{H}\|^2}{M}$ are N and $\frac{2N^2}{M}$, respectively. Therefore, letting $l \leq N$, we derive

$$P \left\{ \frac{\|\mathbf{h}_k^H \Phi \mathbf{H}\|^2}{M} \leq l \right\} = P \left\{ \frac{\|\mathbf{h}_k^H \Phi \mathbf{H}\|^2}{M} - N \leq (l - N) \right\} \quad (96)$$

$$\leq P \left\{ \left| \frac{\|\mathbf{h}_k^H \Phi \mathbf{H}\|^2}{M} - N \right| \geq (N - l) \right\} \quad (97)$$

$$\leq \frac{2N^2}{M(N - l)^2}, \quad (98)$$

where (98) is due to Chebychev inequality. By the extreme value theory [21], we obtain

$$P \left\{ \min_{k=1, \dots, K} \frac{\|\mathbf{h}_k^H \Phi \mathbf{H}\|^2}{M} \geq l \right\} = P \left\{ \frac{\|\mathbf{h}_k^H \Phi \mathbf{H}\|^2}{M} \geq l \right\}^K \quad (99)$$

$$= \left(1 - P \left\{ \frac{\|\mathbf{h}_k^H \Phi \mathbf{H}\|^2}{M} \leq l \right\} \right)^K. \quad (100)$$

Then, combining the (98) and (100), it is obtained that

$$P \left\{ \min_{k=1, \dots, K} \frac{\|\mathbf{h}_k^H \Phi \mathbf{H}\|^2}{M} \geq l \right\} = \left(1 - \frac{2N^2}{M(N - l)^2} \right)^K \rightarrow \exp \left(- \frac{\frac{K}{M} 2N^2}{(N - l)^2} \right), \quad (101)$$

as $K \rightarrow \infty$. It is obvious that the lower bound of $\mathbb{E}\{C^*\}$ is given as

$$\mathbb{E}\{C^*\} \geq \mathbb{E} \log \left(1 + P_{\max} \min_{k=1, \dots, K} \frac{\|\mathbf{h}_k^H \Phi \mathbf{H}\|^2}{M} \right) \quad (102)$$

$$\geq P \left\{ \min_{k=1, \dots, K} \frac{\|\mathbf{h}_k^H \Phi \mathbf{H}\|^2}{M} \geq l \right\} \log(1 + lP_{\max}) \rightarrow \exp \left(- \frac{\frac{K}{M} 2N^2}{(N - l)^2} \right) \log(1 + lP_{\max}), \quad (103)$$

as $K \rightarrow \infty$, where (103) is due to (101). From (103), it is easy to see that since $l < N$ and $\frac{K}{M} \leq \infty$ is a fixed ratio, the lower bound (103) both is $O(1)$ for the fixed N and $N \rightarrow \infty$ cases. Next, we show the upper bound of $\mathbb{E}\{C^*\}$. For the minimum received signal noise ratio (SNR),

we obtain

$$\max_{\mathcal{Q}} \min_{k=1, \dots, K} \mathbf{h}_k^H \Phi \mathbf{H} \mathbf{Q} \mathbf{H}^H \Phi^H \mathbf{h}_k \quad (104)$$

$$\leq \frac{1}{K} \max_{\mathcal{Q}} \sum_{k=1}^K \mathbf{h}_k^H \Phi \mathbf{H} \mathbf{Q} \mathbf{H}^H \Phi^H \mathbf{h}_k \quad (105)$$

$$= \frac{1}{K} \max_{\mathcal{Q}} \sum_{k=1}^K \text{Tr} (\mathbf{Q} \mathbf{H}^H \Phi^H \mathbf{h}_k \mathbf{h}_k^H \Phi \mathbf{H}) \quad (106)$$

$$= \frac{1}{K} \max_{\mathcal{Q}} \text{Tr} \left(\mathbf{Q} \sum_{k=1}^K \mathbf{H}^H \Phi^H \mathbf{h}_k \mathbf{h}_k^H \Phi \mathbf{H} \right) \quad (107)$$

$$= \frac{1}{K} \max_{\mathcal{Q}} \text{Tr} (\mathbf{Q} \boldsymbol{\Omega} \boldsymbol{\Omega}^H) \quad (108)$$

$$= \frac{P_{\max}}{K} \lambda_{\max} (\boldsymbol{\Omega} \boldsymbol{\Omega}^H), \quad (109)$$

where $\boldsymbol{\Omega} = [\mathbf{H}^H \Phi^H \mathbf{h}_1, \mathbf{H}^H \Phi^H \mathbf{h}_2, \dots, \mathbf{H}^H \Phi^H \mathbf{h}_K]$; (105) is due to the fact that the minimum received SNR is upper bounded by the average received SNR; (109) is due to the fact that the maximization (108) is equivalent to maximum eigenvalue of the matrix $\lambda_{\max} (\boldsymbol{\Omega} \boldsymbol{\Omega}^H)$ [18]. From the the eigenvalue of random matrix theory [22], it is obtained that due to $\Psi_{m,k} \sim \mathcal{CN}(0, N)$ (Please notice that $\Psi_{m,k}$ is elements of matrix $\boldsymbol{\Omega}$), we obtain

$$\frac{P_{\max}}{K} \lambda_{\max} (\boldsymbol{\Omega} \boldsymbol{\Omega}^H) \rightarrow P_{\max} \left(N + N \sqrt{\frac{M}{K}} \right)^2, \quad (110)$$

a.s., as $K \rightarrow \infty$, $M \rightarrow \infty$ and $\frac{K}{M} < \infty$, which implies $C^* \leq \log \left(1 + P_{\max} \left(N + N \sqrt{\frac{M}{K}} \right)^2 \right)$, and it follows $\mathbb{E} \{C^*\} \leq O(1)$ for the fixed N case, and $\mathbb{E} \{C^*\} \leq O(\log(N^2))$ for the $N \rightarrow \infty$ case.

REFERENCES

- [1] E. Basar, M. Di Renzo, J. De Rosny, M. Debbah, M. Alouini, and R. Zhang, “Wireless communications through reconfigurable intelligent surfaces,” *IEEE Access*, vol. 7, pp. 116 753–116 773, Aug. 2019.
- [2] C. Huang, G. C. Alexandropoulos, C. Yuen, and M. Debbah, “Indoor signal focusing with deep learning designed reconfigurable intelligent surfaces,” in *Proc. IEEE 20th International Workshop on SPAWC*, Jul. 2019, pp. 1–5.
- [3] C. Liaskos, A. Tsoliaridou, A. Pitsillides, S. Ioannidis, and I. F. Akyildiz, “Using any surface to realize a new paradigm for wireless communications,” *arXiv:1806.04585*, Jun. 2018. [Online]. Available: <http://arxiv.org/abs/1806.04585>
- [4] W. Qingqing and R. Zhang, “Towards smart and reconfigurable environment: Intelligent reflecting surface aided wireless networks,” *arXiv:1905.00152*, Aug. 2019. [Online]. Available: <http://arxiv.org/abs/1905.00152>

- [5] S. Hu, F. Rusek, and O. Edfors, "Beyond massive mimo: The potential of data transmission with large intelligent surfaces," *IEEE Trans. Signal Process.*, vol. 66, no. 10, pp. 2746–2758, May 2018.
- [6] Y. Han, W. Tang, S. Jin, C. Wen, and X. Ma, "Large intelligent surface-assisted wireless communication exploiting statistical csi," *IEEE Trans. Veh. Technol.*, vol. 68, no. 8, pp. 8238–8242, Aug. 2019.
- [7] Q. Wu and R. Zhang, "Intelligent reflecting surface enhanced wireless network: Joint active and passive beamforming design," in *Proc. IEEE GLOBECOM*, Dec. 2018, pp. 1–6.
- [8] S. Li, B. Duo, X. Yuan, Y.-C. Liang, M. Di Renzo *et al.*, "Reconfigurable intelligent surface assisted uav communication: Joint trajectory design and passive beamforming," *arXiv:1908.04082*, Dec. 2019. [Online]. Available: <http://arxiv.org/abs/1908.04082>
- [9] K. Ntontin, M. Di Renzo, J. Song, F. Lazarakis, J. de Rosny, D.-T. Phan-Huy, O. Simeone, R. Zhang, M. Debbah, G. Leroosey *et al.*, "Reconfigurable intelligent surfaces vs. relaying: Differences, similarities, and performance comparison," *arXiv:1908.08747*, Aug. 2019. [Online]. Available: <http://arxiv.org/abs/1908.08747>
- [10] Q. Wu and R. Zhang, "Intelligent reflecting surface enhanced wireless network via joint active and passive beamforming," *IEEE Trans. Wireless Commun.*, pp. 1–1, 2019, early access.
- [11] Y. Li, M. Jiang, Q. Zhang, and J. Qin, "Joint beamforming design in multi-cluster miso noma intelligent reflecting surface-aided downlink communication networks," *arXiv:1909.06972*, Sep. 2019. [Online]. Available: <http://arxiv.org/abs/1909.06972>
- [12] C. Huang, A. Zappone, G. C. Alexandropoulos, M. Debbah, and C. Yuen, "Reconfigurable intelligent surfaces for energy efficiency in wireless communication," *IEEE Trans. Wireless Commun.*, vol. 18, no. 8, pp. 4157–4170, Aug. 2019.
- [13] Y. Tang, G. Ma, H. Xie, J. Xu, and X. Han, "Joint transmit and reflective beamforming design for irs-assisted multiuser miso swipt systems," *arXiv preprint arXiv:1910.07156*, Oct. 2019.
- [14] J. Zhao, "Optimizations with intelligent reflecting surfaces (irss) in 6g wireless networks: Power control, quality of service, max-min fair beamforming for unicast, broadcast, and multicast with multi-antenna mobile users and multiple irss," *arXiv:1908.03965*, Aug. 2019. [Online]. Available: <http://arxiv.org/abs/1908.03965>
- [15] N. Jindal and Z. Luo, "Capacity limits of multiple antenna multicast," in *Proc. IEEE ISIT*, Jul. 2006, pp. 1841–1845.
- [16] "Cisco visual networking index: Global mobile data traffic forecast update, 2017-2022 white paper," San Jose, CA, USA, Feb. 2019.
- [17] B. Zhou, Y. Cui, and M. Tao, "Optimal dynamic multicast scheduling for cache-enabled content-centric wireless networks," *IEEE Trans. Commun.*, vol. 65, no. 7, pp. 2956–2970, Jul. 2017.
- [18] S. Boyd and L. Vandenberghe, *Convex optimization*. Cambridge, UK: Cambridge university press, 2004.
- [19] Y. Liang, V. V. Veeravalli, and H. Vincent Poor, "Resource allocation for wireless fading relay channels: Max-min solution," *IEEE Trans. Inf. Theory*, vol. 53, no. 10, pp. 3432–3453, Oct. 2007.
- [20] S. Markov, "An iterative method for algebraic solution to interval equations," *Applied Numerical Mathematics*, vol. 30, no. 2-3, pp. 3432–3453, Oct. 1999.
- [21] M. Fisz and R. Bartoszyński, *Probability theory and mathematical statistics*. New York, YN, USA: J. wiley, 2018.
- [22] J. W. Silverstein, "The smallest eigenvalue of a large dimensional wishart matrix," *The Annals of Probability*, vol. 13, no. 4, pp. 1364–1368, 1985.